Finite-dimensional observers for port-Hamiltonian systems of conservation laws

Paul Kotyczka, Henning Joos, Yongxin Wu and Yann Le Gorrec

***Abstract*— We consider the port-Hamiltonian formulation of systems of two conservation laws with canonical interdomain coupling in one spatial dimension. Based on the structure-preserving discretization in space and time, we propose two directions for the estimation of the discrete states from boundary measurement. First, we design full state Luenberger observers for the linear case. To guarantee unconditional asymptotic stability of the discrete-time error system, special attention is paid to the implementation of the correction term in the sense of implicit damping injection. Second, we exploit the flatness of the considered class of possibly nonlinear hyperbolic systems, which is preserved under the applied geometric discretization schemes, to obtain a state estimation based on boundary measurement. Numerical experiments serve as a basis for the comparison and discussion of the two proposed discrete-time estimation schemes for hyperbolic conservation laws.**

I. INTRODUCTION

In order to implement state feedback control, observer design is necessary for the lack of complete state measurement in real physical applications. Deterministic observer design for linear finite dimensional systems has been established in the 60s and 70s by Luenberger [1]. However, in the nonlinear and infinite dimensional cases, observer design is still an open research problem. In last two decades, a powerful modeling and control approach, called *port-Hamiltonian* (PH) approach has been proposed to cope with nonlinear and distributed parameter systems. Based on the energy and a structured representation of the power flows and dissipation in the system, the PH framework is particularly suited to describe the complex behavior of multi-physical systems [2]. The PH approach has been generalized to infinite-dimensional systems described by partial differential equations (PDEs) in [3], [4]. Observer design for finite-dimensional PH systems has been investigated in the last ten years. It has been shown that the passivity of PH systems is very useful for the observer design [5]. The idea of *Interconnection and Damping Assignment* has been extended to the observer design for PH systems in [6], [7].

In the infinite-dimensional case, particular attention has to be paid to numerical issues associated with the design and implementation of finite dimensional observers. Recently, progress has been made on the structure preserving spatial discretization of PH systems, applicable to arbitrary spatial dimension and complex geometries [8], [9]. A definition of *discrete-time* PH systems based on time discretization with collocation methods, which extends the notion of symplectic integration schemes to open systems, has been proposed in [10]. The simplest approach, which leads to such a discrete-time PH system is the *symplectic Euler* scheme, applied to partitioned systems. In [11], it is shown that beyond the preservation of the PH structure, also the flatness property of the corresponding outputs is preserved, which allows for the explicit computation of discrete-time feedforward controls.

In this paper, we present two state estimation schemes based on the full structure preserving discretization of hyperbolic systems of conservation laws. First, we present Luenberger type observers based on *implicit* damping injection with *collocated* and *non-collocated* measurements. Second, we exploit the *flatness* of the discrete-time finite-dimensional approximate models to construct an *explicit* scheme for state estimation.

The paper is structured as follows. Section II gives an overview of 1D PH systems of conservation laws and their structure preserving discretization in space and time. The main results of the paper, the implicit damping injection based observer and the flatness-based state estimation, are introduced in Section III. In Section IV, we show the effectiveness of the proposed observers on the benchmark example of the 1D wave equation, for which the solution is exactly known. At last, we conclude this paper with final remarks and some future perspectives.

II. PRELIMINARIES

A. Port-Hamiltonian systems of conservation laws

We consider 1D systems of two conservation laws in PH form, written in terms of exterior differential calculus[1]. According to [3], the PDE representation can be split into *structure*, *dynamics* and *constitutive equations*,

$$\begin{bmatrix} f^p \\ f^q \end{bmatrix} = \begin{bmatrix} 0 & \mathrm{d} \\ \mathrm{d} & 0 \end{bmatrix} \begin{bmatrix} e^p \\ e^q \end{bmatrix}, \qquad \text{(Structure)} \qquad (1a)$$

$$\begin{bmatrix} \dot{p} \\ \dot{q} \end{bmatrix} = \begin{bmatrix} -f^p \\ -f^q \end{bmatrix}, \qquad \text{(Dynamics)} \qquad (1b)$$

$$\begin{bmatrix} e^p \\ e^q \end{bmatrix} = \begin{bmatrix} \delta_p H \\ \delta_q H \end{bmatrix}. \qquad \text{(Constit. Eq.)} \qquad (1c)$$

Considering an open domain $\Omega = (0, L)$, the *state* differential forms $p, q \in L^2\Lambda^1(\Omega) \subset \mathbb{R}$ represent the conserved

[1] See [12] for an introduction to differential forms.

This work was supported by the Agence Nationale de la Recherche/Deutsche Forschungsgemeinschaft (ANR-DFG) project INFIDHEM, ID ANR-16-CE92-0028.

P. Kotyczka and H. Joos are with the Department of Mechanical Engineering, Technical University of Munich, 85748 Garching, Germany kotyczka@tum.de, henning.joos@tum.de

Y. Wu and Y. Le Gorrec are with FEMTO-ST Institute, AS2M Department, Univ. Bourgogne Franche-Comté, Univ. de Franche-Comté/CNRS/ENSMM, 25000 Besançon, France yongxin.wu@femto-st.fr, legorrec@femto-st.fr

quantities. *Flows* $f^p, f^q \in L^2\Lambda^1(\Omega)$ and *efforts* (or co-states) $e^p, e^q \in H^1\Lambda^0(\Omega)$ represent *dual*, *power-conjugated port* variables. The *exterior derivative* $\mathrm{d} : \Lambda^0(\Omega) \to \Lambda^1(\Omega)$ as a unifying differential operator in exterior calculus plays the role of the spatial derivative in 1D. $\delta_p H$ and $\delta_q H$ are the *variational* derivatives[2] of the *energy* or *Hamiltonian functional* $H = \int_0^L \mathcal{H}$ with the Hamiltonian density $\mathcal{H} : \Lambda^1(\Omega) \times \Lambda^1(\Omega) \times \Omega \to \Lambda^1(\Omega)$. With the definition of *boundary inputs*, i. e. imposed boundary conditions (BCs)

$$\begin{bmatrix} u_1 \\ u_2 \end{bmatrix} = \begin{bmatrix} e^q(0) \\ e^p(L) \end{bmatrix} \qquad \text{(Input BCs)} \qquad (2)$$

and the collocated power-conjugate outputs

$$\begin{bmatrix} y_1 \\ y_2 \end{bmatrix} = \begin{bmatrix} e^p(0) \\ -e^q(L) \end{bmatrix}, \qquad \text{(Coll. outputs)} \qquad (3)$$

the application of the generalized Stokes' theorem yields the *structural* balance equation

$$\int_0^L e^p \wedge f^p + \int_0^L e^q \wedge f^q + y_1 u_1 + y_2 u_2 = 0. \qquad (4)$$

In 1D, the *exterior product* $\wedge : \Lambda^0(\Omega) \times \Lambda^1(\Omega) \to \Lambda^1(\Omega)$ of a 0-form (function) with a 1-form simply coincides with the scalar product. After substitution of (1b) and (1c), one obtains the energy balance

$$\dot{H} = y_1 u_1 + y_2 u_2, \qquad (5)$$

which shows that the considered class of systems (assuming H to be bounded from below) is *passive*, even *lossless*.

In this paper, we consider linear constitutive equation of the form $e^p = *p$, $e^q = *q$, which represents a linear wave equation with speed of propagation $c = 1$. The result for flatness-based state estimation can be extended, with the appropriate discretization of the constitutive equations[3] in a straightforward manner to nonlinear hyperbolic systems like the Saint Venant equations or the Euler equations of isentropic gas flow [13].

In some applications, the measured output is different from the power-conjugated output[4]. We shall see how to use such kind of information in the observer design.

B. Structure-preserving spatial discretization

The structure-preserving discretization of the system (1), (2), (3) with mixed Whitney finite elements according to [8] (with a flow mapping parameter $\alpha = 0$) yields the state representation[5]

$$\begin{gathered}\begin{bmatrix} -f^p \\ -f^q \end{bmatrix} = \begin{bmatrix} 0 & D \\ -D^T & 0 \end{bmatrix} \begin{bmatrix} e^p \\ e^q \end{bmatrix} + \begin{bmatrix} g_1 & 0 \\ 0 & g_2 \end{bmatrix} \begin{bmatrix} u_1 \\ u_2 \end{bmatrix}, \\ \begin{bmatrix} y_1 \\ y_2 \end{bmatrix} = \begin{bmatrix} e_1^p \\ -e_N^q \end{bmatrix}\end{gathered} \qquad (6)$$

with the discretized flow and effort vectors $f^p = [f_1^p, \dots, f_N^p]$, $f^q = [f_1^q, \dots, f_N^q]$, $e^p = [e_1^p, \dots, e_N^p]$ and $e^q = [e_1^q, \dots, e_N^q]$ and the matrices

$$D = \begin{bmatrix} -1 & & & \\ 1 & -1 & & \\ & \ddots & \ddots & \\ & & 1 & -1 \end{bmatrix}, \; g_1 = \begin{bmatrix} 1 \\ 0 \\ \vdots \\ 0 \end{bmatrix}, \; g_2 = \begin{bmatrix} 0 \\ \vdots \\ 0 \\ -1 \end{bmatrix}. \qquad (7)$$

The discrete flows $f_i^p = -\dot{p}_i$, $f_i^q = -\dot{q}_i$ are the negative time derivatives of the lumped states $\tilde{p}_i = p_i$ and $\tilde{q}_i = q_i$, $i = 1, \dots, N$, which have the interpretation of *integral* conserved quantities over the discretization edges. e_i^p, e_i^q denote the approximations of the nodal efforts (co-states), with $e_0^q = u_1$ and $e_{N+1}^p = u_2$ the boundary inputs. It is straightforward to verify from the (skew-)symmetry of this state representation that the discretized structural balance equation

$$\sum_{i=1}^N e_i^p f_i^p + \sum_{i=1}^N e_i^q f_i^q + y_1 u_1 + y_2 u_2 = 0 \qquad (8)$$

holds, which approximates (4).

In the case of a linear wave equation on the interval $\Omega = (0, 1)$ with Hamiltonian density $= \frac{1}{2} p \wedge *p + \frac{1}{2} q \wedge *q$, which is treated as en example in the paper, the consistent effort approximation is given by

$$e_i^p = \frac{p_i}{\Delta z}, \quad e_i^q = \frac{q_i}{\Delta z}, \qquad \Delta z = \frac{1}{N}. \qquad (9)$$

C. Structure-preserving discretization in time

With the *symplectic Euler scheme*, the simplest possible structure-preserving time integration method[6] is applied to the finite-dimensional approximation (6). The result is

$$\begin{gathered}\frac{1}{\Delta t} \begin{bmatrix} p^{k+1} - p^k \\ q^{k+1} - q^k \end{bmatrix} = \frac{1}{\Delta z} \begin{bmatrix} 0 & D \\ -D^T & 0 \end{bmatrix} \begin{bmatrix} p^{k+1} \\ q^k \end{bmatrix} + \begin{bmatrix} g_1 & 0 \\ 0 & g_2 \end{bmatrix} \begin{bmatrix} u_1^k \\ u_2^{k+1} \end{bmatrix} \\ \begin{bmatrix} y_1^{k+1} \\ y_2^k \end{bmatrix} = \frac{1}{\Delta z} \begin{bmatrix} g_1^T & 0^T \\ 0^T & g_2^T \end{bmatrix} \begin{bmatrix} p^{k+1} \\ q^k \end{bmatrix}.\end{gathered} \qquad (10)$$

The inputs are sampled according to their physical character, consistent with the symplectic Euler scheme, i. e. $u_1^k = e_0^{q,k}$ and $u_2^{k+1} = -e_{N+1}^{p,k+q}$. With the definition of the outputs, we obtain an approximation of the energy balance of the form

$$\frac{1}{\Delta t} \begin{bmatrix} e^{p,k+1} & e^{q,k} \end{bmatrix} \begin{bmatrix} p^{k+1} - p^k \\ q^{k+1} - q^k \end{bmatrix} = (y_1^{k+1})^T u_1^k + (y_2^k)^T u_2^{k+1}. \qquad (11)$$

For a more general definition of discrete-time Dirac structures/PH systems, and the discussion of the discrete-time (structural) energy balance, we refer to the recent paper [10]. Flatness of the considered class of discretized models and discrete-time trajectory generation is treated in [11].

III. Finite-dimensional state observers

We use the fully discretized model of the wave equation (10) for the design of two different observers in the sequel. The output vector is written in terms of the two sampling instants k and $k + 1$, according to the occurrence in the discrete balance equation (10).

[2] For the definition, see [2], p. 232.

[3] In the spirit of [11].

[4] Consider as an example the laser measurement of the displacement at the end of a flexible structure.

[5] The same equations are obtained with finite volumes on regularly staggered grids [14].

[6] See [15] for geometric numerical integration of Hamiltonian systems.

A. Luenberger observer

For the observer design we consider two different application cases. First, the observer is designed from the measured collocated output according to (10). Second, the case of non-collocated measurement is investigated. If the considered wave equation represents the dynamics of deflection $w(z,t)$ of a string, the boundary measurement

$$y_m = \int_0^1 q(z,t)\,dz = w(1,t) - w(0,t) \tag{12}$$

with $q = \frac{\partial w}{\partial z}$ corresponds to the total deflection, which can be easily measured by a laser sensor in an experimental setup.

An interesting issue, which requires some care in the design of the full state observer is the fact that the model (10) is not in the form $x^{k+1} = Ax^k + Bu^k$, $y^k = Cx^k$ of an (explicit) discrete-time linear system. Instead, due to the use of the symplectic Euler scheme, the difference equations are partially implicit.

1) Observer based on collocated measurement: We concentrate on the observer design using the collocated output as shown in (10). We set up the following copy of the system, including the correction term. The sampling instants, at which the output error is evaluated, are written α and β.

$$\frac{1}{\Delta t}\begin{bmatrix}\hat{p}^{k+1}-\hat{p}^k\\ \hat{q}^{k+1}-\hat{q}^k\end{bmatrix} = \frac{1}{\Delta z}\begin{bmatrix}0 & D\\ -D^T & 0\end{bmatrix}\begin{bmatrix}\hat{p}^{k+1}\\ \hat{q}^k\end{bmatrix} + \begin{bmatrix}g_1 & 0\\ 0 & g_2\end{bmatrix}\begin{bmatrix}u_1^k\\ u_2^{k+1}\end{bmatrix} + \begin{bmatrix}l_1 & 0\\ 0 & l_2\end{bmatrix}\left(\begin{bmatrix}y_1^\alpha\\ y_2^\beta\end{bmatrix} - \begin{bmatrix}\hat{y}_1^\alpha\\ \hat{y}_2^\beta\end{bmatrix}\right) \tag{13}$$

$$\begin{bmatrix}\hat{y}_1^{k+1}\\ \hat{y}_2^k\end{bmatrix} = \frac{1}{\Delta z}\begin{bmatrix}g_1^T & 0^T\\ 0^T & g_2^T\end{bmatrix}\begin{bmatrix}\hat{p}^{k+1}\\ \hat{q}^k\end{bmatrix}.$$

The choice of α and β, is crucial for the unconditional asymptotic stability[7] of the observer error dynamics ($\tilde{p}^k = \hat{p}^k - p^k$, $\tilde{q}^k = \hat{q}^k - q^k$)

$$\begin{bmatrix}I & 0\\ cD^T & I\end{bmatrix}\begin{bmatrix}\tilde{p}^{k+1}\\ \tilde{q}^{k+1}\end{bmatrix} = \begin{bmatrix}I & cD\\ 0 & I\end{bmatrix}\begin{bmatrix}\tilde{p}^k\\ \tilde{q}^k\end{bmatrix} - \begin{bmatrix}cl_1 g_1^T & 0\\ 0 & cl_2 g_2^T\end{bmatrix}\begin{bmatrix}\tilde{p}^\alpha\\ \tilde{q}^\beta\end{bmatrix}, \tag{14}$$

where $c = \frac{\Delta t}{\Delta z} > 0$ denotes the ratio of time and spatial discretization step.

Proposition 1: The error system (14) with $l_1 = r_1 g_1$, $l_2 = r_2 g_2$, $r_1, r_2 > 0$, is unconditionally asymptotically stable for $c \leq 1$ and the choice $\alpha = \beta = k+1$.

Proof: For the given choices, Eq. (14) becomes

$$\begin{bmatrix}I + cR_1 & 0\\ cD^T & I + cR_2\end{bmatrix}\begin{bmatrix}\tilde{p}^{k+1}\\ \tilde{q}^{k+1}\end{bmatrix} = \begin{bmatrix}I & cD\\ 0 & I\end{bmatrix}\begin{bmatrix}\tilde{p}^k\\ \tilde{q}^k\end{bmatrix} \tag{15}$$

with $R_1, R_2 \geq 0$ matrices of rank 1, which justifies the designation "damping injection observer". For $R_1 = R_2 = 0$, the eigenvalues of the generalized eigenvalue problem (E, A) associated with (15) lie on the unit circle for $0 < c \leq 1$. The proof for $c = 1$ is shown in the appendix, for $c = 0$ all eigenvalues are 1, for $0 < c < 1$, the eigenvalues are distributed between these extrema on the unit circle. Depending on whether α and β are k or $k+1$, the damping matrices appear either on the right or the left hand side of (15). The former case corresponds to damping injection with the explicit, the latter with the implicit Euler scheme, which is known to be unconditionally numerically stable. From asymptotic stability of the corresponding continuous time observer error dynamics[8], and the unconditional numerical stability of the discrete time implementation, the unconditional asymptotic stability of (15) follows. ■

[7]The equilibrium of the discrete-time model is *unconditionally* asymptotically stable if it is asymptotically stable for arbitrary ration $c = \frac{\Delta t}{\Delta z}$.

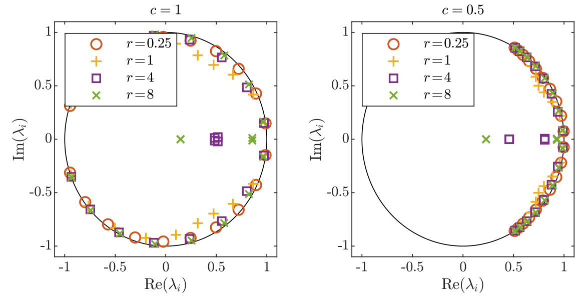

Fig. 1. Eigenvalues of (E, A), implicit observer damping injection.

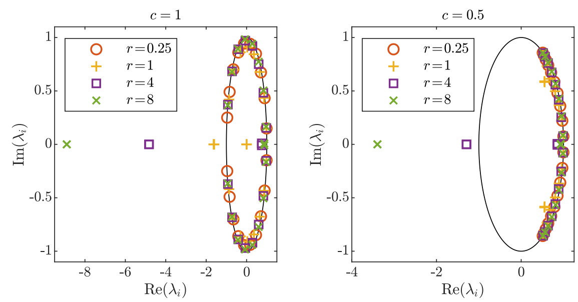

Fig. 2. Eigenvalues of (E, A), explicit observer damping injection.

Figures 1 and 2 illustrate the effects of implicit and explicit damping injection to the locations of the eigenvalues of (E, A). For explicit damping injection, the eigenvalues leave the unit circle above a certain threshold of $r_1 = r_2 = r$, depending on c. In the implicit case, the eigenvalues remain confined to the unit circle.

Remark 1: Figure 3 justifies the possibility of implicit damping injection in a digital control system. If the cycle times for the tasks "read measurement data" (1), "update observer (and controller)" (2) and "set reference values" (3) are small compared to the main cycle time, the knowledge of y_1^{k+1} and y_2^{k+1} can be assumed for the computation of $\hat{p}^{k+1}$ and $\hat{q}^{k+1}$.

2) Observer based on non-collocated measurement: We now consider observer design with a measurement (12). The

[8]The introduced damping is pervasive and the corresponding system eigenvalues lie in $\mathbb{C}^-$.

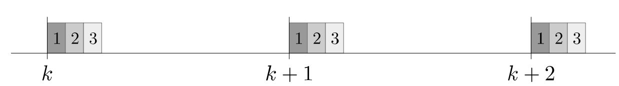

Fig. 3. Task cycles in a simplistic digital control system without communication delays

spatial and time discretization of this output is given by

$$y_m^{k+1} = \frac{1}{\Delta z}\begin{bmatrix} g_3^T & 0 \end{bmatrix}\begin{bmatrix} p^{k+1} \\ q^k \end{bmatrix} \tag{16}$$

with $g_3^T = \begin{bmatrix}1, \ldots, 1\end{bmatrix} \in \mathbb{R}^N$. We propose an observer based on this non-collocated output (16) under the following form:

$$\begin{aligned} \frac{1}{\Delta t}\begin{bmatrix} \hat{p}^{k+1} - \hat{p}^k \\ \hat{q}^{k+1} - \hat{q}^k \end{bmatrix} &= \frac{1}{\Delta z}\begin{bmatrix} 0 & D \\ -D^T & 0 \end{bmatrix}\begin{bmatrix} \hat{p}^{k+1} \\ \hat{q}^k \end{bmatrix} + \begin{bmatrix} g_1 & 0 \\ 0 & g_2 \end{bmatrix}\begin{bmatrix} u_1^k \\ u_2^{k+1} \end{bmatrix} \\ &\quad + \begin{bmatrix} l_3 \\ 0 \end{bmatrix}(y_m^\alpha - \hat{y}_m^\alpha) \\ \hat{y}_m^{k+1} &= \frac{1}{\Delta z}\begin{bmatrix} g_3^T & 0^T \end{bmatrix}\begin{bmatrix} \hat{p}^{k+1} \\ \hat{q}^k \end{bmatrix}. \end{aligned} \tag{17}$$

The observer error dynamics with $c = \frac{\Delta t}{\Delta z} > 0$ is

$$\begin{bmatrix} I & 0 \\ cD^T & I \end{bmatrix}\begin{bmatrix} \tilde{p}^{k+1} \\ \tilde{q}^{k+1} \end{bmatrix} = \begin{bmatrix} I & cD \\ 0 & I \end{bmatrix}\begin{bmatrix} \tilde{p}^k \\ \tilde{q}^k \end{bmatrix} - \begin{bmatrix} cl_3 g_3^T & 0 \\ 0 & 0 \end{bmatrix}\begin{bmatrix} \tilde{p}^\alpha \\ \tilde{q}^\beta \end{bmatrix}. \tag{18}$$

Proposition 2: The error system (18) with $l_3 = r_3 g_3$, is unconditionally asymptotically stable for $c \leq 1$ and the choice $\alpha = k+1$.

Proof: With $\alpha = k+1$, Eq. (18) becomes Eq. (15) with $R_3 = r_3 g_3 g_3^T \geq 0$ a matrix of rank 1 and $R_2 = 0$. Then the proof follows the same way as the one of Proposition 1. ■

B. Flatness-based state estimation

We exploit the flatness of the fully discretized system model (10) for the design of an observer. Flatness of (10) and its implication for the *explicit* computation of feedforward control trajectories has been studied in [11]. Flatness of discrete-time systems [16] and of hyperbolic systems [17] are characterized in an analogous way, by the ability to express states and inputs in terms of forward and backward shifts of the outputs. Therefore, the fully discretized model (10) – in contrast to only semi-discretization in space – is adequate for feedforward control, but also for the state estimation of the hyperbolic systems.

To obtain estimates $\hat{p}^l$ and $\hat{q}^l$ for the discrete states of the wave equation at time $k = l$, based on current and past boundary inputs and measurements, we consider the single equations of the fully discretized model (10) for $i = 1, \ldots, N$

$$p_i^{k+1} = p_i^k + \frac{\Delta t}{\Delta z}(q_{i-1}^k - q_i^k), \tag{A1}$$

$$q_i^{k+1} = q_i^k + \frac{\Delta t}{\Delta z}(p_i^{k+1} - p_{i+1}^{k+1}), \tag{B1}$$

where

$$\begin{aligned} q_0^k &= \Delta z u_1^k, \\ p_{N+1}^k &= \Delta z u_2^k, \end{aligned} \quad \text{and} \quad \begin{aligned} p_1^k &= \Delta z y_1^k, \\ q_N^k &= -\Delta z y_2^k. \end{aligned} \tag{20}$$

Depending on which data on the spatio-temporal grid is known, Eqs. (A1) and (B1) can be solved for different

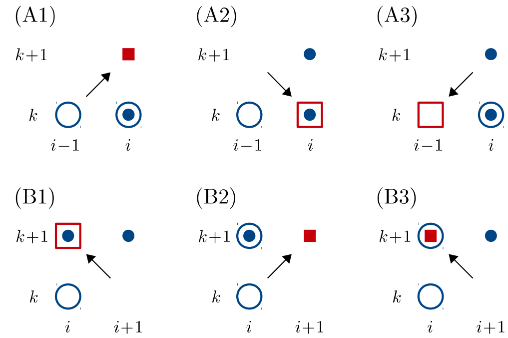

Fig. 4. Computation of states on the spatio-temporal grid based on the update equations for p (first row) and q (second row). Blue circles denote given data, red squares the computed quantity. Filled objects stand for p, empty objects for q. The arrows indicate the information flow.

variables, e. g.

$$q_i^k = q_{i-1}^k - \frac{\Delta z}{\Delta t}(p_i^{k+1} - p_i^k), \tag{A2}$$

$$q_{i-1}^k = q_i^k + \frac{\Delta z}{\Delta t}(p_i^{k+1} - p_i^k), \tag{A3}$$

$$p_{i+1}^{k+1} = p_i^{k+1} - \frac{\Delta z}{\Delta t}(q_i^{k+1} - q_i^k), \tag{B2}$$

$$p_i^{k+1} = p_{i+1}^{k+1} + \frac{\Delta z}{\Delta t}(q_i^{k+1} - q_i^k). \tag{B3}$$

The six (out of 8) indicated possibilities are depicted in Fig. 4, where red squares stand for the unknowns and blue circles stand for given data. The p and q variables are represented as solid or empty objects, respectively.

Assuming the knowledge of boundary inputs and measured outputs, the unknown states can be estimated by a two phase explicit scheme. We assume an even number of discretization intervals and define $M = \frac{N}{2}$:

Given:
- Inputs $u_1^{l-1}, \ldots, u_1^{l-N+1}$, $u_2^l, \ldots, u_2^{l-N+2}$.
- Outputs $y_1^l, \ldots, y_1^{l-N+1}$, $y_2^l, \ldots, y_2^{l-N+1}$.

Phase 1:
- Evaluate (A2) with $i = 1$ and (B3) with $i = N$.
- For $j = 1$ to $M - 1$ do:
  - Eval. (B2) with $i = j$ and (A3) with $i = N - j + 1$.
  - Eval. (A2) with $i = j + 1$ and (B3) with $i = N - j$.

Phase 2:
- Evaluate (B1) with $k = l - M$.
- For $k = l - M + 1$ to $l - 1$ do:
  - Evaluate (A1).
  - Evaluate (B1).

Result:
- Estimates $\hat{p}_2^l, \ldots, \hat{p}_N^l$ and $\hat{q}_1^l, \ldots, \hat{q}_{N-1}^l$.

Remark 2: Calling the algorithm to obtain the state estimates at $k = l$ "flatness-based" is justified as follows. Define the boundary inputs as additional outputs. Then the algorithm sketched above leads to a representation of the system states and inputs in terms of the outputs and their time shifts.

Remark 3: Although we presented the algorithm for the case of the linear wave equation, it can be applied for an explicit state estimation also in the nonlinear case. The key

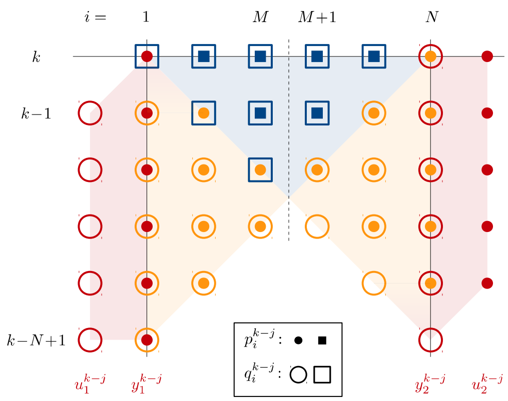

Fig. 5. Schematic of the state estimation at instant k: Starting with the boundary in- and outputs (red), in a first phase (yellow) the update equations are solved according to A2/B2 from the left and B3/A3 from the right to obtain a representation of past states in terms of the boundary port variables. In a second phase (blue), the current state estimation is obtained by solving the update equations according to B1/A1.

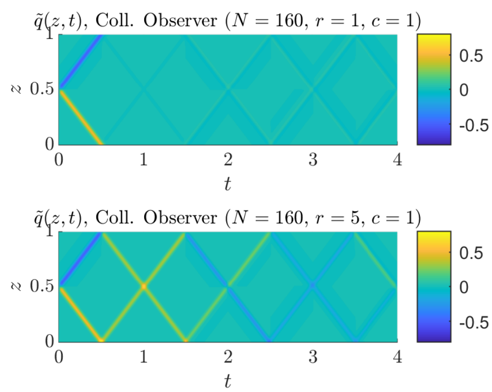

Fig. 6. Surface plots of the estimation error $\tilde{q}$ for $c = 1$, $N = 160$ and two different values of r.

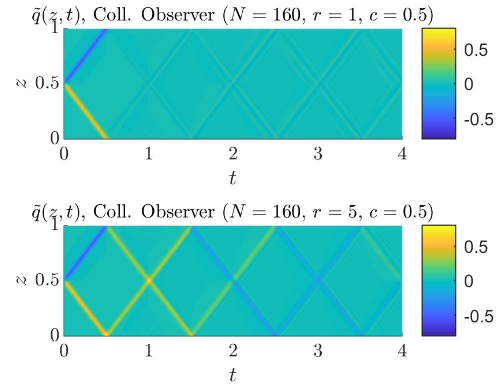

Fig. 7. Surface plots of the estimation error $\tilde{q}$ for $c = \frac{1}{2}$, $N = 160$ and two different values of r.

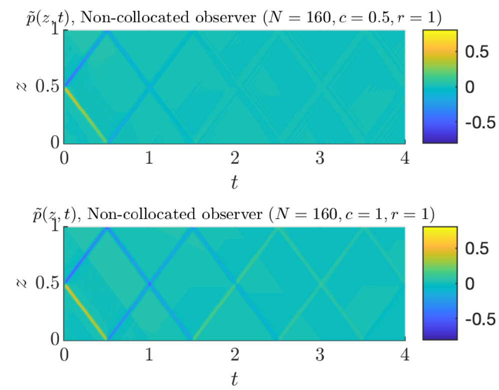

Fig. 8. Surface plots of estimation errors with non-collocated measurement, $N = 160$, $c = 1$ and $c = \frac{1}{2}$.

for the applicability to the nonlinear case is an appropriate consistent approximation of the constitutive equations, which allows for the transport of information through the spatio-temporal grid as sketched in Figures 4 and 5 for the linear case. See for this issue also [11], where the approximation of the constitutive equations is instrumental in deriving the flatness-based feedforward control.

IV. Numerical Example and Discussion

To assess the estimation of the distributed states of the wave equation using the presented techniques, we consider the linear wave equation on $\Omega = (0, 1)$ with homogeneous boundary conditions $u_1 = u_2 = 0$. The exact solution can be obtained according to d'Alambert and is composed of left and right travelling waves, which are reflected at the boundaries with and without a change in sign. We study initial conditions

$$p(z, 0) = e^{-\frac{(z-0.5)^2}{0.025^2}} \quad \text{and} \quad q(z, 0) = 0. \tag{22}$$

A. Damping injection observer

Figures 6 to 8 display the errors $\tilde{q}(z,t) = \hat{q}(z,t) - q(z,t)$ between the exact solution and the estimated states[9] for the Luenberger observers with different values $r \in \{1, 5\}$ and $c \in \{1, \frac{1}{2}\}$ of the observer parameter and the ratio of temporal and spatial step. In the case of collocated measurement, $r = 1$ has the effect of a *absorbing* boundary condition for the error system, which brings the estimation error (up to a bounded residual due to discretization) to zero in finite time. This effect does not appear for a different value of r in and also in the case of distributed measurement, see Fig. 8. In these cases, the observer corrections cannot be interpreted in terms of perfectly absorbing boundary condition, which leads to an asymptotic decay of the estimation error.

B. Flatness-based estimation

The flatness-based estimation of the state with the presented algorithm leads to the expected convergence in finite time (again up to the bounded discretization error) of the estimation error, see Fig. (9). An advantage of this approach is that, with the appropriate approximation of the constitutive equations, it is applicable to nonlinear conservation laws. A remarkable effect is the occurrence of an oscillating error

[9] The plots for $\tilde{p}(z,t)$ show qualitatively the same results and are omitted.

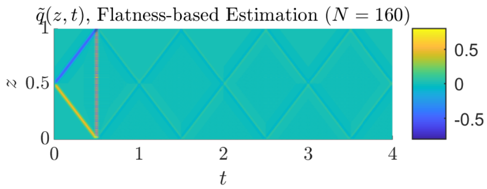

Fig. 9. Surface plots of estimation errors, $N = 160$, $c = 1$.

of rather high magnitude around $t = \frac{1}{2}$, which is distributed over the whole spatial domain. It strongly motivates the study of a improved implementation of the numerical scheme for state estimation.

V. CONCLUSIONS AND FUTURE WORK

We presented the application of two different to tackle the state estimation problem in infinite-dimensional port-Hamiltonian systems of conservation laws. We departed from the structure-preserving discretization of the equations in space and time, and followed first the classical Luenberger observer approach and second the notion of flatness in hyperbolic/discrete-time systems.

Future work will be concerned with the embedding of the finite-dimensional observers in the closed loop, the numerical error analysis, guarantees for closed-loop error bounds and the application of the flatness-based state estimation to nonlinear systems ov conservation laws.

REFERENCES

[1] D. Luenberger, "An introduction to observers," *IEEE Transactions on automatic control*, vol. 16, no. 6, pp. 596–602, 1971.

[2] V. Duindam, A. Macchelli, S. Stramigioli, and H. Bruyninckx, *Modeling and Control of Complex Physical Systems: The Port-Hamiltonian Approach*. Springer Science & Business Media, 2009.

[3] A. J. van der Schaft and B. M. Maschke, "Hamiltonian formulation of distributed-parameter systems with boundary energy flow," *Journal of Geometry and Physics*, vol. 42, no. 1, pp. 166–194, 2002.

[4] Y. Le Gorrec, H. Zwart, and B. Maschke, "Dirac structures and boundary control systems associated with skew-symmetric differential operators," *SIAM journal on control and optimization*, vol. 44, no. 5, pp. 1864–1892, 2005.

[5] A. Venkatraman and A. van der Schaft, "Full-order observer design for a class of port-hamiltonian systems," *Automatica*, vol. 46, no. 3, pp. 555–561, 2010.

[6] B. Vincent, N. Hudon, L. Lefèvre, and D. Dochain, "Port-hamiltonian observer design for plasma profile estimation in tokamaks," *IFAC-PapersOnLine*, vol. 49, no. 24, pp. 93–98, 2016.

[7] B. Biedermann, P. Rosenzweig, and T. Meurer, "Passivity-based observer design for state affine systems using interconnection and damping assignment," in *2018 IEEE Conference on Decision and Control (CDC)*, pp. 4662–4667, Dec 2018.

[8] P. Kotyczka, B. Maschke, and L. Lefèvre, "Weak form of Stokes-Dirac structures and geometric discretization of port-Hamiltonian systems," *Journal of Computational Physics*, vol. 361, pp. 442–476, 2018.

[9] V. Trenchant, H. Ramírez, Y. Le Gorrec, and P. Kotyczka, "Finite differences on staggered grids preserving the port-Hamiltonian structure with application to an acoustic duct," *Journal of Computational Physics*, vol. 373, pp. 673–697, 2018.

[10] P. Kotyczka and L. Lefèvre, "Discrete-time port-Hamiltonian systems: A definition based on symplectic integration," *arXiv preprint arXiv:1811.07852*, 2018.

[11] P. Kotyczka, "Discrete-time flatness-based feedforward control for the shallow water equations," in *11th IFAC Symposium on Nonlinear Control Systems (NOLCOS) (submitted)*, 2019.

[12] H. Flanders, *Differential forms with applications to the physical sciences*. Academic Press, New York, 1963.

[13] P. J. Morrison, "Hamiltonian description of the ideal fluid," *Reviews of Modern Physics*, vol. 70, no. 2, pp. 467–521, 1998.

[14] P. Kotyczka, "Finite volume structure-preserving discretization of 1D distributed-parameter port-Hamiltonian systems," *IFAC-PapersOnLine*, vol. 49, no. 8, pp. 298–303, 2016.

[15] E. Hairer, C. Lubich, and G. Wanner, *Geometric Numerical Integration: Structure-Preserving Algorithms for Ordinary Differential Equations*, vol. 31. Springer Science & Business Media, 2006.

[16] H. Sira-Ramírez and S. K. Agrawal, *Differentially flat systems*. Marcel Dekker, Inc., 2004.

[17] F. Woittennek, "On flatness and controllability of simple hyperbolic distributed parameter systems," in *18th IFAC World Congress, Milano*, pp. 14452–14457, 2011.

[18] J. R. Silvester, "Determinants of block matrices," *The Mathematical Gazette*, vol. 84, no. 501, pp. 460–467, 2000.

APPENDIX

We investigate the stability of $Ex^{k+1} = Ax^k$ with

$$E = \begin{bmatrix} I & 0 \\ cD^T & I \end{bmatrix}, \quad A = \begin{bmatrix} I & cD \\ 0 & I \end{bmatrix}, \tag{23}$$

where $c > 0$ is a constant and $D = -D^T$ as given in (7).

Lemma 1: For $c = 1$, the eigenvalues of the generalized eigenvalue problem (E, A) are $e^{\pm j\theta_i}$ with $\theta_i = (i - \frac{1}{2})\frac{2\pi}{2N+1}$.

Proof: The eigenvalues of the generalized eigenvalue problem given by the discrete-time dynamics $Ex^{k+1} = Ax^k$ are the roots of

$$\det(A - E\lambda) = \begin{vmatrix} (1-\lambda)I & cD \\ -\lambda c D^T & (1-\lambda)I. \end{vmatrix} \tag{24}$$

By commutativity of the matrices in the second row, we can use the formula given in [18], which yields

$$\det(A - E\lambda) = \det((1-\lambda)^2 I + c\lambda DD^T). \tag{25}$$

The determinant of the tridiagonal matrix

$$\begin{vmatrix} (1-\lambda)^2 + 2c\lambda & -c\lambda & & \\ -c\lambda & \ddots & \ddots & \\ & \ddots & (1-\lambda)^2 + 2c\lambda & -c\lambda \\ & & -c\lambda & (1-\lambda)^2 + c\lambda \end{vmatrix} \tag{26}$$

is obtained by recursion. For $c = 1$, the characteristic polynomial is

$$\begin{aligned} \sum_{i=0}^{2N} (-1)^i \lambda^i &= 1 + \sum_{i=1}^{N} \lambda^{2i} - \sum_{i=1}^{N} \lambda^{2i-1} \\ &= 1 + (\lambda^2 - \lambda) \sum_{i=0}^{N-1} \lambda^{2i} = \frac{1 + \lambda^{2N+1}}{1 + \lambda}, \end{aligned} \tag{27}$$

where we exploited $\sum_{i=0}^{n-1} r^i = \frac{1-r^n}{1-r}$. The roots, which due to $\lambda \neq -1$ must be conjugate complex numbers $\lambda_i = e^{\pm j\theta_i}$, have to satisfy

$$e^{\pm j\theta_i(2N+1)} = e^{j\pi(2i-1)} = -1, \quad i = 1, \ldots N, \tag{28}$$

from which $\theta_i = (i - \frac{1}{2})\frac{2\pi}{2N+1}$ follows. ∎

Note that with $\Delta t = \frac{1}{N}$, the continuous-time counterparts $\pm\frac{1}{\Delta t}\theta_i j = \pm\frac{(2i-1)}{2+\frac{1}{N}}\pi j$ of the discrete-time eigenvalues converge for $N \to \infty$ to the exact locations $\pm\frac{2i-1}{2}\pi j$ of the eigenvalues of the wave equation under homogeneous boundary conditions on u_1 and u_2.